

COMPARATIVE MODELLING AND SCENARIO ANALYSIS OF SECTOR-COUPLED ISLAND ENERGY SYSTEM OPTIMISATIONS

Victor Breburda^{1,2}, Peter-Philipp Schierhorn¹, Simon Massat², Benjamin Blat-Belmonte², Ekehard Tröster¹, Stephan Rinderknecht²

¹*Energynautics GmbH, Robert-Bosch-Straße 7, Darmstadt, Germany*

²*Institute for Mechatronic Systems – Technical University Darmstadt, Otto-Berndt-Straße 2, Darmstadt, Germany*

Keywords: DISPATCH OPTIMISATION, SECTOR COUPLING, OFF-GRID ISLAND ENERGY SYSTEM, PIECEWISE LINEAR MODELLING, DUNKELFLAUTE EVENTS

Abstract

Dispatch optimisations of an off-grid island energy system were carried out. These optimisations compared a linear and piecewise linear efficiency modelling approaches for sector couplers, different *Dunkelflaute* weather scenarios; and different horizon lengths over one year with an hourly resolution. Solar and wind power are complemented by battery and hydrogen storages, along with sector couplers: electrolyser, fuel cell, gas turbine and steam boiler to meet electricity and high-temperature heat loads. The unit dispatch optimisations were conducted in PyPSA. The piecewise linear model showed a concentration of the operation points at maximum efficiency for the electrolyser, which can be operated more flexibly than the other components. When modelled with constant efficiency, the gas turbine showed a significantly higher electricity output. The fuel cell and the steam boiler did not show significant differences, between the two modelling approaches. The relatively minor influence of horizon length underscored the importance of thorough pre-optimisation strategies, particularly in anticipating and managing *Dunkelflaute* events, where long-term foresight is crucial for system resilience. A four-week *Dunkelflaute* showed that the capacity of the EL in conjunction with the availability of electricity from RE in the period before the *Dunkelflaute* was the limiting factor for bridging the *Dunkelflaute*.

1 Introduction

In view of the increasing global demand for energy, the expansion of distribution grids and the development of renewable energy systems have become a central problem. Due to the significant investment cost of building renewable energy structures, the main interest from an energy system design perspective and long-term capacity planning is to select the most economically and/or lowest CO₂ emissions viable alternative [1]. This complex problem is addressed in numerous papers using mixed integer linear programming (MILP) and includes the allocation of energy resources and services as well as capacity expansion plans with minimised system costs, maximised system reliability and increased energy security [1]. The integration of fluctuating renewable energy (RE) sources into power systems requires short-term dispatch planning and new, more accurate optimisation techniques and modelling of power systems and individual units [1] to keep system reliability and stability.

In this work, short-term dispatch optimisations of an island system were carried out for a time horizon of one year with an hourly resolution. The focus of this research was the comparison of linear and piecewise linear models used for the sector couplers between electricity, heat and hydrogen considering different parameters and weather scenarios. First, Chapter 2 describes the weather conditions, the electricity load

and the heat load as well as, the system components. These consist of the RE sources: photovoltaics (PV) and wind turbines (WT); the sector couplers: an electrolyser (EL), a fuel cell (FC), a gas turbine (GT) and a steam boiler (SB); and storage technologies: a battery energy storage system (BESS) and a hydrogen tank (H2T). Chapter 3 describes the methodology used in the optimisations, the different modelling approaches for the individual components and their efficiency curves as well as the different horizon and weather scenarios under which the optimizations were run. Chapter 4 presents a comparison of the dispatch behaviour under the different rolling horizons, the two efficiency modelling approaches and weather scenarios. For this, the resilience of the system to reduced availability of RE generation in so-called *Dunkelflaute* events is discussed. Chapter 5 gives a summary and a conclusion of the results.

2 Problem formulation and system description

2.1 Island System and Boundary Conditions

The system used in the simulations is a virtual island system supplied by only renewable energy with an electrical load and a heat load. The weather data is from the Caribbean Island of Andros in the Bahamas (24.64° N, 77.00° W). This location was chosen as it has sufficient availability of both solar irradiation and wind power to provide for even conditions in

the optimisation [2]. The electrical peak load is 36.66 MW_{el}, the average load is 25.41 MW_{el} and the total annual electricity consumption is ~223 GWh_{el}. The peak load occurs every day at around 18:00 h. The load drops slightly at weekends. Due to the location of the island, there are only minor fluctuations in the electrical load throughout the year due to small temperature variations. The heat peak load is 25 MW_{th}, the average load is 19.45 MW_{th} and the total annual heat demand is ~170 GWh_{th}. The heat load is highest every day between 6:00 and 18:00 h and drops only slightly at night and weekends. This heat load follows an industrial heat load profile, with only minor fluctuations throughout the year.

A BESS and a H2T are used to store energy. The BESS is intended to serve as hourly or daily storage and the hydrogen as seasonal storage. An EL and a FC serve as sector couplers between electricity and hydrogen. A GT and a SB, which use hydrogen as fuel, are used to cover the high-temperature heat load. The GT produces electricity as well as heat, thus coupling hydrogen with heat and electricity simultaneously.

2.2 System components

2.2.1 Power Generators: They are comprised of PV panels and wind turbines. PV plays an important role in supplying remote regions [3]. Its use can significantly reduce dependence on energy imports and electricity generation costs in an isolated system.

Wind energy can be integrated into existing well-interconnected large-scale electricity grids without jeopardising system stability [4]. However, their integration into small electricity grids is more challenging [4].

2.2.2 Sector Couplers: Hydrogen is a promising alternative to decarbonise the electricity, heat and industry sectors. It can be produced through water electrolysis through RE sources in an EL [5]. Pure hydrogen is currently rarely utilized for covering electricity needs [5], but FCs have a high efficiency at partial load and are therefore well suited for flexible operation in conjunction with variable renewable energies [6]. In contrast, the use of hydrogen in heat supply is more widespread [5]. Therefore, the sector couplers selected for this research were an EL and a FC for the electricity sector and a GT and a SB for the industrial and heat sectors.

For the EL and FC under study, the proton exchange membrane technology was selected. These have a high efficiency at partial load, which makes them ideal for a comparison of the two efficiency models used in this research [6].

GTs in power generation are currently mainly operated by burning methane (CH₄) [8]. As GTs have short start-up times and high operational flexibility [9], they are relevant in modern and future energy systems. Therefore, it is important to reduce their CO₂ emissions [8]. Alongside the use of synthetic fuels, the combustion of green hydrogen (H₂) is the most promising way to decarbonize gas turbine fuels [8]. Similarly, SBs are

used to provide high-temperature steam for industrial processes and can potentially be decarbonized by using green hydrogen [5].

2.2.3 Energy Storages: The power available from solar and wind power depends on the weather. Using energy storages is required to provide a temporal shift of power to keep the system in operation. The system uses a BESS and a H2T.

BESS are widely used in RE power island systems for hourly or daily storage, peak load reduction, frequency control and other grid-supporting measures [10] due to their different advantages [11]. Since no conventional generation units were planned for grid stabilization in the island scenario, this role was taken over by the BESS and/or the GT.

Hydrogen was intended to be used as seasonal storage in the examined scenarios. Compression technology is best suited for this, as it is well-developed and offers fast charge and discharge rates [12].

3 Methodology

A MILP problem was formulated considering a time horizon of one year in hourly resolution. The optimisation was conducted for various lengths of rolling horizons, two sector coupler efficiency modelling approaches and several *Dunkelflaute* scenarios. The inputs of the optimisation were:

- Meteorological data: Irradiance, temperature and wind speeds at the aforementioned specified coordinates
- Load curves: Residential electricity load and industrial high-temperature heat load
- Unit characteristics and costs: Efficiency curves, operational limitations and costs for PV panels, WT, EL, FC, GT, SB, BESS and H2T

The decision variables were:

- Unit commitment status of the piecewise linear segments of the EL, the FC, the GT and the SB
- Input and output power of the EL, the FC, the GT and the SB
- Curtailment of PV panels and WT
- Energy content of the BESS and the H2T

The system consisted of three buses, one for electricity, one for hydrogen and one for high-temperature heat. The power balance on each bus had to be fulfilled at any timestep t :

$$P_{PV,t} + P_{WT,t} + P_{GT,out,el,t} + P_{BESS,out,t} + P_{FC,out,t} \\ = P_{load,el,t} + P_{BESS,in,t} + P_{EC,in,t},$$

$$P_{EC,out,t} + P_{H2T,out,t} \\ = P_{H2T,in,t} + P_{GT,in,t} + P_{SB,in,t} \\ + P_{FC,in,t},$$

$$P_{GT,out,heat,t} + P_{SB,out,t} = P_{load,heat,t},$$

with $P_{n,in/out,t}$ representing the power output or input of the component n in the timestep t . The objective function, which was set to be minimised, equalled the sum of unit operation costs of all timesteps:

$$f_{\text{objective}} = \sum_{t,n} P_{n,out,t} c_n,$$

where c_n is the marginal cost.

3.1 Modelling of units

3.1.1 PV panels: The approach for calculating the power from a solar panel used in this work is also used in the simulation software HOMER Pro [13] and in numerous papers [14–16]. This model follows:

$$P_{PV,t} = P_{PV, \text{rated}} \frac{G_t}{G_{STC}} [1 + \gamma(T_{\text{cell},t} - T_{\text{cell},STC})],$$

where irradiation under standard test conditions $T_{\text{cell},STC} = 25^\circ\text{C}$ is $G_{STC} = 1 \text{ kW/m}^2$ and the temperature coefficient is $\gamma = -0.48\%/^\circ\text{C}$ [13]. G_t corresponds to the irradiation at time t . The cell temperature is calculated according to

$$T_{\text{cell},t} = T_{\text{ambient},t} + \frac{G_t}{G_{NOCT}} (T_{\text{cell},NOCT} - T_{\text{ambient},NOCT}),$$

where $G_{NOCT} = 0.8 \text{ kW/m}^2$ corresponds to the irradiation at which the PV module reaches the nominal operating cell temperature (NOCT). $T_{\text{ambient},t}$ represents the ambient temperature. $T_{\text{ambient},NOCT} = 20^\circ\text{C}$ and $T_{\text{cell},NOCT} = 46.5^\circ\text{C}$ apply [13].

3.1.2 WT: The output power of the WT was calculated from the wind speed using the power curve:

$$P_{WKA,t}(v) = P_{\text{rated}} \left(\frac{v_t^k - v_{ci}^k}{v_r^k - v_{ci}^k} \right),$$

with the wind speed v_t , the cut-in speed v_{ci} , the rated speed v_r , the cut-out speed v_{co} , the rated power P_{rated} and the order k of the power curve [17]. A value of $k=1.4$ was used for the modelling [17], according to the dimensions of the WT AAER A1500-80, which has a rated power of $P_{\text{rated}} = 1.5 \text{ MW}$ and a hub height of 80 meters [18]. Between nominal wind speed and cut-out speed, the power is equal to the nominal power. Below the cut-in speed and above the cut-out speed, the WT does not produce any electricity [17].

3.1.3 Sector Couplers: In the literature, sector couplers are usually modelled using linear [15] or piecewise linear approximation (PWA) to approximate the non-linear behaviour of units [6,19–21].

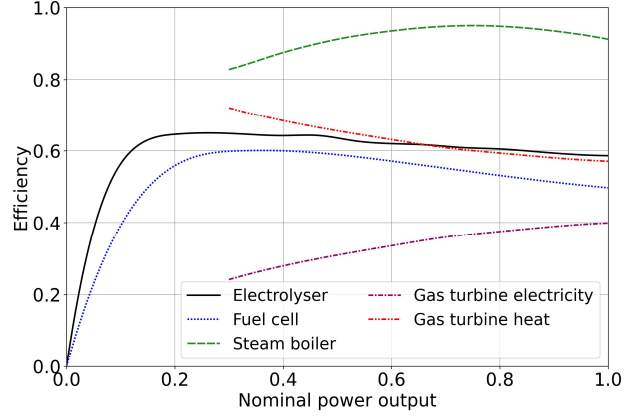


Figure 1: Efficiency curves of sector couplers [6,22–24]

From the efficiency curves shown in Figure 1 the power curve was calculated according to

$$P_{SC,out} = P_{SC,in} \eta_{SC}$$

and for the GT additionally

$$P_{GT,out,heat} = P_{GT,in} (1 - \eta_{GT,el}) \eta_{GT,heat}$$

The power curves were approximated by a PWA. The number and placement of the segments were optimised by minimization of the Residual Sum of Squares (RSS) at various tolerances. The power output of the segment i interpolated between the point (x_i, y_i) and (x_{i+1}, y_{i+1}) is given by

$$P_{SC,out,PWA,i} = \alpha_i (P_{SC,in} - 1) + y_i$$

with the slope of the i -th segment being

$$\alpha_i = \frac{y_{i+1} - y_i}{x_{i+1} - x_i}$$

and the operational range of the segment being limited by

$$x_i \leq P_{SC,in} \leq x_{i+1}$$

3.1.4 Energy Storage Systems: The modelling of the operation of energy storage systems is carried out to different degrees of detail in the literature. Alberizzi (2020) [3] specifies storage capacity and maximum discharge capacity and does not take standing losses or ageing of the BESS into account. The cyclical ageing of a BESS is non-linear but is usually modelled linearly, as in Marroco (2021) [19]. Cyclical ageing can also be considered temperature-dependent. This type of modelling is non-linear and therefore not suitable for use with MILP [19,25].

The BESS and the H2T were modelled with an energy balance:

$$e_{S,t} = \eta_{S,stand} e_{S,t-1} + \eta_{S,in} P_{S,in,t} - \eta_{S,out}^{-1} P_{S,out,t}$$

$\eta_{S,stand}$ represents the standing losses due to e.g. electrical discharge overtime or leakage. The efficiencies of power going in and out of the storage S are given by

$$\eta_{S,in} = \eta_{S,out} = \sqrt{\eta_{S,round\ trip}}$$

where $\eta_{BESS,round\ trip} = 90\%$ [26] and $\eta_{H2T,round\ trip} = 85\%$ apply for the individual storage units [12]. The BESS energy content $e_{BESS,t}$ is additionally limited by

$$0.3E_{BESS} \leq e_{BESS,t} \leq 0.9E_{BESS}$$

where E_{BESS} is the total storage capacity to prevent damage and increased ageing of the battery [11]. A value of 5% per month is assumed for standing losses for the BESS [27]. Cyclical ageing is considered linearly in the form of marginal costs for discharging the BESS. This assumption is only valid if the depth of discharge is not too large. For the H2T no restrictions regarding the depth of discharge were considered, standing losses and cyclical ageing are low and were neglected.

3.1.5 Dispatch costs: The dispatch costs for all units are shown in Table 1. As curtailment of RE is expected in the scenario, WTs are typically curtailed before PV due to their slightly higher marginal costs compared to the virtually negligible marginal costs associated with PV production. Therefore, assigning marginal costs to WT helps establish a clear order of curtailment for optimisation purposes. The marginal cost for the EL is assumed to be the same as the FC, and likewise for the SB and the GT. The marginal cost of the GT was increased by a factor of 1.3 according to Öberg (2022) [28].

Table 1: Components marginal cost in USD per dispatched MWh

	PV	WT	EL	FC	GT	SB	BESS	H2T
c_n	0	0.5	6.84	6.84	8.37	8.37	6.01	0
	[29]			[29]	[29]			

3.2 Dispatch optimisation

The unit sizes for the dispatch optimisation were determined in a preliminary capacity optimisation, which assumed constant efficiencies for all sector couplers. For the dispatch optimisation, on the other hand, the sector couplers' efficiency curves were modelled as an optimisation variable. The implementation of these efficiency curves significantly increases the complexity and computational effort of the model. Therefore, a rolling horizon is used to optimise the dispatch of the specified periods sequentially to reduce the optimisation problem complexity and computational time. Since the H2T is intended to be used as seasonal storage beyond the length of one horizon, it is necessary to perform a pre-optimisation, which determines the state of charge (SOC) of the H2T at the last timestep of each horizon.

$$e_{n,H2T,t=t_{last,disopt}} = e_{n,H2T,t=t_{last,preopt}}$$

A simplified dispatch optimisation with constant efficiencies serves as the pre-optimisation. The initial SOC of the H2T in the first horizon is specified by the pre-optimisation. In all further horizons, the storage level is specified by the solution for the same time step in the respective previous horizon.

Optimisations with the horizon lengths 24, 48, 84, 168, 336, 720 and 1095 hours and half a horizon length of overlap were conducted and compared. Due to the small size of the system, it is possible to use such a horizon length. In practice, smaller horizon lengths and a different methodology would be selected for the pre-optimisation, as the computing time is usually significantly higher in these cases due to larger and more complex systems.

For the two efficiency modelling approaches, three cases were compared. One case with constant efficiency and two with a PWA efficiency curve each with different approximation tolerances (1 and 0.1%). These optimisations were performed with a 720-hour horizon length.

To determine resilience against *Dunkelflauten*, dispatch optimisations were carried out for 16 *Dunkelflauten* scenarios lasting from one to four weeks and for a reduction of solar irradiation, wind speeds and temperatures to 90, 70, 50 and 30% of their initial values. The dispatch optimisation for each scenario was carried out with a system capacity of 100, 105, 110, 120, 130 and 140% regarding the capacities from the preliminary capacity optimisation. The start of the *Dunkelflauten* events was set in the middle of the year (time step 4386) as it poses a challenge to the performance capacity of the EL and the storage capacity of the H2T. In this time step, the production of hydrogen was specified by the pre-optimisation and the EL operated at full power if the weather conditions permitted and the H2T was almost full.

4 Results

The optimisation problem was formulated in PyPSA employing HiGHS as the solver. A relative MIP gap of 0.05% and an absolute MIP gap of 200 were imposed. The relative gap is relevant for accuracy at short horizons, the absolute gap is relevant for accuracy at longer horizons. Simulations were performed on a PowerEdge R440 Server with an Intel Xeon Bronze 3104 1,7 GHz and with 32 GB RAM.

4.1 Horizon length

With a system capacity of 100%, a horizon length of 336 hours was required to find a viable dispatch for the entire year. With 105% capacity, a solution required only a horizon length of 48 hours. The system requires either sufficient foresight or additional capacity to compensate for an operating behaviour that deviates from the pre-optimisation due to the different modelling approaches during dispatch optimisation. Figure 2 illustrates a comparison of the different horizon lengths by means of the H2T SOC.

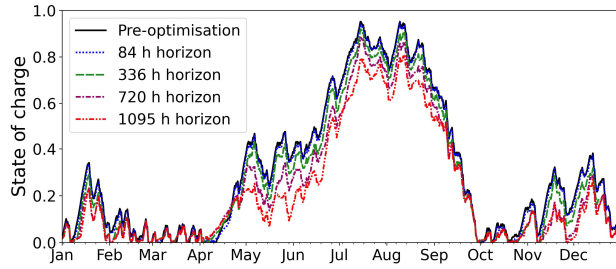


Figure 2: SOC of the H2T at different horizon lengths

It shows an increasing deviation of the SOC in the dispatch optimisation from the pre-optimisation with increasing horizon length. Due to the pre-optimisation, more hydrogen tends to be stored than necessary. With larger horizon lengths, the optimisation is less bound to the specification from the pre-optimisation and thus the system can be operated at a lower cost. With longer weather forecasts, it is possible to better plan the electrolyser dispatch and thus operate it at its optimum operating point. This effect is particularly evident in April in the slower filling of the H2T with longer horizons.

4.2 Model comparison

The difference in net electricity generation among the efficiency modelling approaches was examined. Figure 3 shows two spring weeks, which illustrate the differences in electricity dispatch between a constant efficiency and an efficiency curve modelled with 1% tolerance.

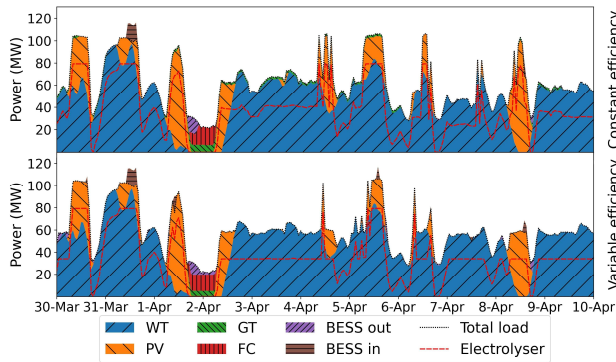


Figure 3: Electricity dispatch comparison for constant efficiency and efficiency curve during spring-time

It can be observed that the EL with an efficiency curve is operated at the same operating point most of the time, whereas the EL with constant efficiency does not show a clear pattern in operation. This is due to the higher efficiency of the EL at approx. 43% load. Since the curtailment of RE was not penalized, i.e. has a zero marginal cost, and the operation of the EL has a marginal cost associated with it, the EL was operated at maximum efficiency if possible. Conversely, in the constant efficiency case, there is no incentive to operate the EL at a specific operating point. Therefore, RE-curtailment was 21.15% for the constant efficiency case compared to 24.27% when using the efficiency curve approach. Optimum operation

of the EL is not always possible. For example, to bridge the *Dunkelflaute* during the night of April 2, the EL is operated at a higher output and thus at a lower efficiency on the preceding days. Figure 4 shows the concentration of operating points of the EL at kink points of the power and efficiency curve.

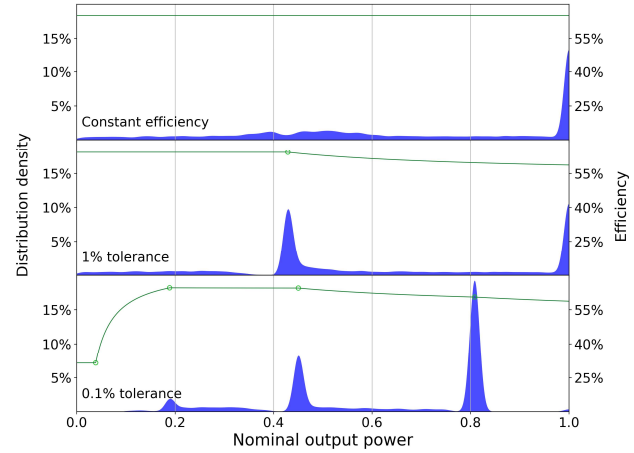


Figure 4: Distribution density of operating points of the EL (blue) with corresponding efficiency curves and kinks (green)

The concentration at the kink points result in operation with the higher efficiency. The EL is hardly operated at full power at a tolerance of 0.1%. The decreasing EL efficiency at partial load below 20% is only reflected at a tolerance of 0.1%. As a result, the EL is no longer operated at partial loads below 20%. However, those phenomena only have a minor effect on the operating costs. A concentration of the operating points also occurs in the case of the fuel cell, although it must be noted that it cannot be operated as flexibly as the EL. The distribution densities of the GT do not differ significantly between the modelling approaches. This is due to the heat-load-dictated operation. The GT acts almost exclusively as a peak load generator for heat load, with the steam boiler covering the base load. The amounts of heat generated in the GT throughout the year hardly differ. At constant efficiency, 19.08 GWh_{el} of electricity and 35.41 GWh_{th} of heat are generated. When modelling with an efficiency curve, these values are 4.03 GWh_{el} for electricity and 34.32 GWh_{th} for heat. The deviation in the amount of electricity produced is due to the modelling of the electrical efficiency and the heat ratio. With constant efficiency, the heat ratio is also constant. When using the efficiency curve, the heat ratio decreases with increasing electricity output. This means that significantly less electricity is produced for the same amount of heat. In some cases, the GT is operated at full load. This operating state only occurs if the ratio of electricity to heat load is similar to the power-to-heat ratio of the GT or if a peak heat load requires it. Although thermal efficiency is lower at full load, operation can be advantageous if electricity is also required as a "by-product".

4.3 Dunkelflauten

Figure 5 shows that short or light *Dunkelflauten* events can be managed with 5 to 20% of additional installed capacity. If the

power provided by RE decreases or the length of the event increases, significant excess capacity is required to cover all loads.

	100%	90%	70%	50%	30%
Weeks of <i>Dunkelflaute</i> 1	100%	105%	120%	130%	140%
Weeks of <i>Dunkelflaute</i> 2	100%	110%	130%	> 140%	> 140%
Weeks of <i>Dunkelflaute</i> 3	100%	110%	130%	> 140%	> 140%
Weeks of <i>Dunkelflaute</i> 4	100%	120%	> 140%	> 140%	> 140%

Figure 5: Required additional capacity for *Dunkelflauten* of various durations and reductions of RE power input

The operating behaviour during various *Dunkelflauten* events was examined based on the energy content of the hydrogen storage system. The levels of the storage content are the same before the *Dunkelflauten* and virtually identical at a given distance after the end of the *Dunkelflauten*. The trends begin to diverge just under two weeks before the start of the *Dunkelflaute*. In the case of the two- and three-week *Dunkelflaute*, significantly more hydrogen is produced up to the start of the *Dunkelflaute* than in the scenario without *Dunkelflaute*. During the first week of the *Dunkelflauten*, the storage SOC continues to increase in all four scenarios.

The full capacity of the H2T is not fully utilized in any scenario. In practice, the H2T would always be as fully charged as possible to have sufficient energy available in scenarios such as this one. In all scenarios, hydrogen is also used as a daily storage during and after the *Dunkelflauten*. This can be recognized by the jagged profiles of the SOC of the H2T (see Figure 6).

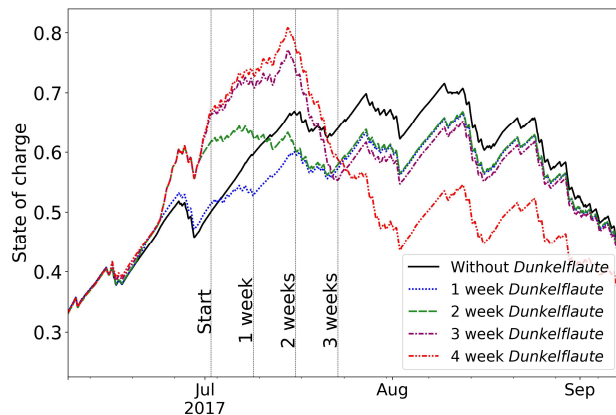


Figure 6: State of charge of the hydrogen storage tank with 70% *Dunkelflaute* and a capacity of 130%

A four-week *Dunkelflaute*, which could only be managed with slack generators, shows that the capacity of the EL in

conjunction with the availability of electricity from RE in the period before the *Dunkelflaute* was the limiting factor for bridging the *Dunkelflaute*. Oversizing of the entire system is not practical. Instead, a capacity optimisation and pre-optimisation of operation were carried out with solar irradiation, wind speeds and temperatures reduced to 70%. These systems can cope with the *Dunkelflauten*. However, this is not due to high overcapacities, but due to the *Dunkelflauten* being considered in the pre-optimisation.

5 Conclusion

The influence of the horizon length on the dispatch of the sector couplers is only minor with a suitable pre-optimisation, whereby the operation of the EL experiences the greatest change due to its flexibility. The model comparison shows that the use of constant efficiencies results in significantly different operating behaviour than using efficiency curves, which incentivises the operation at maximum efficiency. The greatest differences were seen in the flexibly operable EL due to the large hydrogen storage, which acts as a buffer and the GT due to the simultaneous generation of electricity and heat. Modelling with constant efficiency is valid for an initial approximation of operation and is necessary in the case of capacity optimisation. As has been shown, the operating behaviour of units can sometimes deviate significantly when using an efficiency curve. This applies in particular to the EL, which can be operated flexibly using a storage system and to the GT, which couples more than two sectors. The decisive factor was the modelling of the relationship between the two output powers, which in the case of the GT are interdependent. Since in practice, the system would be larger and more complex than this highly simplified system, the costs of operation would not differ significantly with different tolerances and a high tolerance should be selected in these cases. When considering microgrids, which usually consist of only one unit of each type, the use of a low tolerance is recommended. The consideration of *Dunkelflauten* events shows that the system is quite susceptible to changes in weather data. To cope with *Dunkelflauten*, a good forecast or a hydrogen storage tank that is permanently filled is necessary. Therefore, it is recommended that capacity optimisations are not based only on one year's weather data, but rather consider several years and, above all, include extreme weather situations and historical *Dunkelflauten*. Numerous simplifications were made. The results of the optimisation should therefore only be viewed as an approximation.

6 Acknowledgements

We sincerely thank Energynautics GmbH and the Institute for Mechatronic Systems of the Technical University of Darmstadt. for their financial support in conducting this work.

7 References

- [1] Baños, R., Manzano-Agugliaro, F., Montoya, F.G., Gil, C., Alcayde, A., Gómez, J.: 'Optimization methods applied to renewable and sustainable energy: A review',

- Renewable and Sustainable Energy Reviews*, 2011, **15**, (4), pp. 1753–1766
- [2] ‘POWER | Data Access Viewer’, <https://power.larc.nasa.gov/data-access-viewer/>, accessed April, 2024
- [3] Alberizzi, J.C., Rossi, M., Renzi, M.: ‘A MILP algorithm for the optimal sizing of an off-grid hybrid renewable energy system in South Tyrol’, *Energy reports*, 2020
- [4] Ackermann, T.: ‘Wind power in power systems: [... the workshop was entitled "Fourth International Workshop on the Large-Scale Integration of Wind Power and Transmission Networks for Offshore Wind Farms"]’ (Wiley, Chichester, 2005)
- [5] International Energy Agency: ‘The Future of Hydrogen: Seizing today’s opportunities’ (OECD, Paris Cedex 16, 2019)
- [6] Neisen, V., Baader, F.J., Abel, D.: ‘Supervisory Model-based Control using Mixed Integer Optimization for stationary hybrid fuel cell systems’, *IFAC-PapersOnLine*, 2018, **51**, (32), pp. 320–325
- [7] Mohammadi, A., Mehrpooya, M.: ‘A comprehensive review on coupling different types of electrolyzer to renewable energy sources’, *Energy*, 2018, **158**, pp. 632–655
- [8] Noble, D., Wu, D., Emerson, B., Sheppard, S., Lieuwen, T., Angello, L.: ‘Assessment of Current Capabilities and Near-Term Availability of Hydrogen-Fired Gas Turbines Considering a Low-Carbon Future’, *Journal of Engineering for Gas Turbines and Power*, 2021, **143**, (4)
- [9] Kehlhofer, R.: ‘Combined-Cycle Gas & Steam Turbine Power Plants’ (PennWell Books, OnixTransformation.OnixModel.CityOfPublication, 2009)
- [10] ‘Grid-Scale Storage’, <https://www.iea.org/energy-system/electricity/grid-scale-storage>, accessed April, 2024
- [11] Hannan, M.A., Wali, S.B., Ker, P.J., *et al.*: ‘Battery energy-storage system: A review of technologies, optimization objectives, constraints, approaches, and outstanding issues’, *Journal of Energy Storage*, 2021, **42**, p. 103023
- [12] Usman, M.R.: ‘Hydrogen storage methods: Review and current status’, *Renewable and Sustainable Energy Reviews*, 2022, **167**, p. 112743
- [13] ‘HOMER Pro User Manual’, <https://homerenergy.com/pdf/HOMERHelpManual.pdf>
- [14] Li, B., Roche, R., & Miraoui, A.: ‘Microgrid sizing with combined evolutionary algorithm and MILP unit commitment’, *Applied Energy*, 2017, (188), pp. 547–562
- [15] Brandoni, C., Renzi, M.: ‘Optimal sizing of hybrid solar micro-CHP systems for the household sector’, *Applied Thermal Engineering*, 2015, (75), pp. 869–907
- [16] Hwang, J.J., Lai, L.K., Wu, W., Chang, W.R.: ‘Dynamic modeling of a photovoltaic hydrogen fuel cell hybrid system’, *International Journal of Hydrogen Energy*, 2009, **34**, (23), pp. 9531–9542
- [17] Teyabeen, A. A., Akkari, F. R., Jwaid, A. E.: ‘Power Curve Modelling For Wind Turbines’, pp. 179–184
- [18] ‘AAER A1500-70 - 1,50 MW - Wind turbine’, www.wind-turbine-models.com/turbines/597-aaer-a1500-7
- [19] Marocco, P., Ferrero, D., Martelli, E., Santarelli, M., Lanzini, A.: ‘An MILP approach for the optimal design of renewable battery-hydrogen energy systems for off-grid insular communities’, *Energy Conversion and Management*, 2021, **245**, p. 114564
- [20] Marocco, P., Ferrero, D., Lanzini, A., Santarelli, M.: ‘Optimal design of stand-alone solutions based on RES + hydrogen storage feeding off-grid communities’, *Energy Conversion and Management*, 2021, **238**, p. 114147
- [21] Gabrielli, P., Flamm, B., Eichler, A., Gazzani, M., Lygeros, J., Mazzotti, M.: ‘Modeling for Optimal Operation of PEM Fuel Cells and Electrolyzers’
- [22] Erichsen, G., Zimmermann, T., Kather, A.: ‘Effect of Different Interval Lengths in a Rolling Horizon MILP Unit Commitment with Non-Linear Control Model for a Small Energy System’, *Energies*, 2019, **12**, (6), p. 1003
- [23] Short, M., Crosbie, T., Dawood, M., Dawood, N.: ‘Load forecasting and dispatch optimisation for decentralised co-generation plant with dual energy storage’, *Applied Energy*, 2017, **186**, pp. 304–320
- [24] Bartholomy, O.J.: ‘A technical, economic, and environmental assessment of the production of renewable hydrogen from wind in California’ (University of California, Davis, Davis, Calif., 2008)
- [25] Schwarz, C. T., Kapeller, J., & Wimmer, Y.: ‘Techno-Economic Modelling of Stationary Energy Storage Systems with Focus on Temperature’s Influence on Aging’
- [26] ‘Electricity storage and renewables: Costs and markets to 2030’ (International Renewable Energy Agency, [Abu Dhabi], 2017)
- [27] Cui, Y., Du, C., Yin, G., *et al.*: ‘Multi-stress factor model for cycle lifetime prediction of lithium ion batteries with shallow-depth discharge’, *Journal of Power Sources*, 2015, **279**, pp. 123–132
- [28] Öberg, S., Odenberger, M., Johnsson, F.: ‘The value of flexible fuel mixing in hydrogen-fueled gas turbines – A techno-economic study’, *International Journal of Hydrogen Energy*, 2022, **47**, (74), pp. 31684–31702
- [29] ‘2023 Annual Technology Baseline: Technologies Cost and Performance Data for Electricity Generation’, accessed April, 2024